AAS 26-970

GENERALIZED NONLINEAR SPACECRAFT TARGETING WITH IMPLICIT SENSITIVITIES

Quinn P. Moon*, Brandon A. Jones†, and Ryan P. Russell ‡

Solutions to the boundary value problem, traditionally found through numerical shooting methods, are approximated analytically using the higher-order implicit sensitivities of a root-solved process. Existing techniques that improve individual stages of the shooting process are combined with the implicit sensitivities to introduce a generalized predictor-corrector. Using state transition tensors computed along the reference, the generalized predictor-corrector is defined by settings that can be adjusted to emphasize targeting performance or computational cost. The impulsive nonlinear targeting solutions from the generalized predictor-corrector outperform or are comparable to methods in the literature, but are found with less computational effort.

INTRODUCTION

For spacecraft guidance and control, a common targeting strategy steers a spacecraft back to a nominal trajectory or terminal state, solving a Boundary Value Problem (BVP). Analytic first-order targeting solutions, calculated using the State Transition Matrix (STM) [1], provide a computationally light solution ideal for onboard implementation [2]. However, stronger nonlinear dynamics and larger initial state dispersions may justify nonlinear targeting methods. The nonlinear targeting solution $\boldsymbol{u}^*$ connects the dispersed initial state $\delta \boldsymbol{r}_0$ to a reference final state. For two-body dynamics, $\boldsymbol{u}^*$ satisfies the Lambert Problem [3], with neighboring solutions rapidly approximated using first-order expansions [4, 5]. For arbitrary dynamics, $\boldsymbol{u}^*$ has no analytic solution and must be found numerically via shooting methods such as the predictor-corrector [6]. Improvements to the predictor-corrector are made throughout the literature [7–9], but are seldom combined nor produce an analytic solution. The current work combines various contributions from the literature into a single algorithm, dubbed the *generalized predictor-corrector*. Furthermore, though $\boldsymbol{u}^*$ has no analytic solution, its sensitivities are found via the multivariate implicit value theorem, yielding a closed-form approximation.

The multivariate implicit value theorem provides the sensitivities of a root-solved process where the zero of a function is sought that has no analytic solution. Scalar root-solved procedures are ubiquitous in aerospace applications, including Kepler's equation, plane crossings, entries and exits of shadowing regions, and Lambert's boundary value problem. Multivariate root-solved procedures are more complicated. For aerospace applications, Junkins et al. derive the higher-order implicit

*PhD Student, Aerospace Engineering and Engineering Mechanics, quinnpmoon@utexas.edu, http://orcid.org/0000-0002-6766-7577

†Associate Professor, brandon.jones@utexas.edu, http://orcid.org/0000-0003-3480-6320

‡Professor, ryan.russell@austin.utexas.edu, http://orcid.org/0000-0001-7672-0408

sensitivities of a multivariate root-solved process [8]. Turner et al. then develop an automatic-differentiation-based software to efficiently compute the higher-order implicit sensitivities [10]. Differential algebra provides an alternative to analytic expressions of the implicit sensitivities, and has been implemented to solve BVPs using continuous low-thrust maneuvers [11, 12]. Prior work apply the multivariate implicit sensitivities to the initial guess [10, 13] and the correction step [9, 14] of shooting methods.

The majority of existing research on the multivariate implicit value theorem is applied to the optimal control problem. In the current work the scope is extended to include impulsive nonlinear targeting maneuvers. A new higher-order initial guess scheme is derived for the problem, and an alternative derivation for a known higher-order correction step is given. Furthermore, the current work highlights the underappreciated relationship between existing work solving BVPs with State Transition Tensors (STTs) [7, 15] and the implicit value theorem.

The remaining agenda of the current work follows. First, relevant background on STTs and shooting methods is provided based on the existing literature. Second, the generalized predictor-corrector is introduced, incorporating contributions from the literature and the current work as adjustable settings of a single, unified algorithm. Third, the defining settings of the generalized predictor-corrector are discussed individually, with analytic approximations introduced via the implicit value theorem. Lastly, different settings of the generalized predictor-corrector are tested in a case study about Psyche; analytic approximations of the nonlinear targeting solutions are validated against a Monte Carlo study.

RELEVANT BACKGROUND

The current work relies heavily on the theory and application of STTs about a reference trajectory. This section provides an overview of STTs, summarizing contributions from the literature for completeness in the current work [7]. Furthermore, a brief overview of shooting methods and the classic predictor-corrector is provided in the context of the BVP [6].

State Transition Tensors and Einstein Notation

The nonlinear dynamics $\boldsymbol{\phi}$ map an initial state $\boldsymbol{x}_0$ to the final state $\boldsymbol{x}_f$ according to $\boldsymbol{x}_f = \boldsymbol{\phi}(\boldsymbol{x}_0)$. The STTs represent the partials of the flow about a reference trajectory, i.e., the pth-order sensitivity of the final state $\boldsymbol{x}_f$ with respect to the initial state $\boldsymbol{x}_0$ [7]

$$\phi^{i,k_1\cdots k_p} := \frac{\partial x_f^i}{\partial x_0^{k_1} \cdots \partial x_0^{k_p}}. \tag{1}$$

The superscript notation $(i, k_1 \cdots k_p)$ denotes the partial of the ith state with respect to the states k_1 through k_p. The final state dispersion can be approximated with the sth-order Taylor series [7]

$$\delta x_f^i \approx \sum_{p=1}^{s} \frac{1}{p!} \phi^{i,k_1\cdots k_p} \delta x_0^{k_1} \cdots \delta x_0^{k_p}, \tag{2}$$

where repeated indices in the superscript are summed using Einstein's convention. The STTs are propagated with the state along the reference trajectory; the differential equations of the STTs up to fourth-order are presented in [7], and, for completeness, are recorded in Appendix A. The notation in Eq. 1 is expanded to denote the partials of the dynamics with respect to either the position $\boldsymbol{r}$ or velocity $\boldsymbol{v}$. Equation 3, for example, denotes the second-order partial of the ith final position with respect to the jth initial position and the kth initial velocity:

$$\phi_{r,rv}^{i,jk} := \frac{\partial r_f^i}{\partial r_0^j \partial v_0^k}. \tag{3}$$

Shooting Methods and The Classic Predictor-Corrector

Numerous improvements to the predictor-corrector exist throughout the literature, and are combined in the current work to present a unified algorithm. Prior to the presentation of the generalized predictor-corrector, an overview is provided of shooting methods in general; for further reading see [6, 7, 15].

Provided a reference trajectory, solving a BVP entails firing a maneuver that steers an initial position dispersion $\delta \boldsymbol{r}_0$ back to the reference at some final time t_f. The maneuver driving the dispersion back to the reference is denoted as $\boldsymbol{u}^*$. The maneuver $\boldsymbol{u}^*$ is the *numerical* solution of a multivariate root-solved procedure. The most common way to find $\boldsymbol{u}^*$ is through a shooting method, such as the predictor-corrector [6], depicted in Fig. 1. The initial state is propagated to the final time, predicting the final state dispersion $\delta \boldsymbol{r}_f$. The intermediate maneuver $\boldsymbol{u}^{(\rho)}$ is then corrected using a Newton step. The processes of *predicting* the final state dispersion and *correcting* the intermediate solution is repeated until the final target is reached [6] or some maximum iteration q is met.

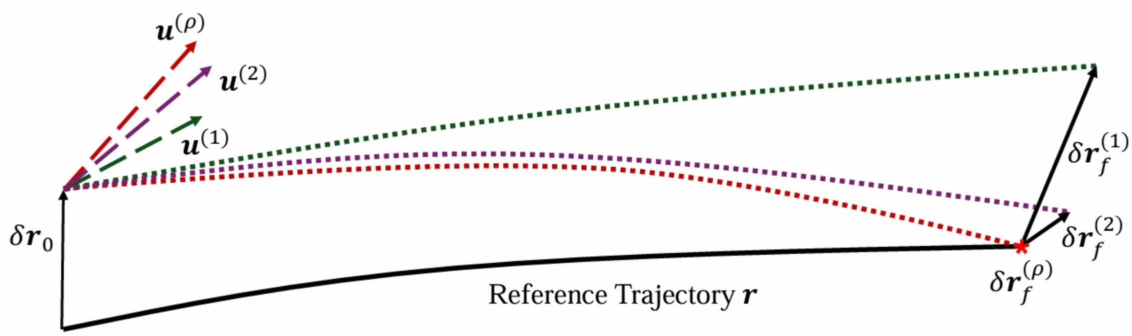

Figure 1: Intermediate solution $\boldsymbol{u}^{(\rho)}$ refined via a shooting method, decreasing the final position dispersion $\delta \boldsymbol{r}_f^{(\rho)}$.

THE GENERALIZED PREDICTOR-CORRECTOR

This work introduces the *generalized predictor-corrector* for solving a BVP by combining key contributions from the literature [7–9] with techniques presented in the current work. The generalized predictor-corrector assumes that the reference STTs are provided to the pth order. The generalized predictor-corrector is defined by five settings $\boldsymbol{\xi} = [\boldsymbol{l}_{(\mathcal{P})}, m, n, q, s]$, depicted in Fig. 2. First, the set of iterations $\boldsymbol{l}$ at which the base STTs $\bar{\bar{\phi}}^{i,k_1\cdots k_{\mathcal{P}}}$ are recomputed to the $\mathcal{P}$th order. The base STTs approximate the STTs used within the correction $\tilde{\phi}^{i,k_1\cdots k_{\mathcal{P}}}$, avoiding costly computations of the STTs at every iteration [16]. Second, the order m of the initial guess $\boldsymbol{u}_{(m)}$ fed into the predictor-corrector. Third, the order n of the correction step $\boldsymbol{c}_{(n)}$ based on the multivariate series reversion [9, 14]. Fourth, the maximum number of iterations q. Fifth, the order s of the dynamics $\boldsymbol{\phi}_{(s)}$ used to predict the final state dispersion $\delta \boldsymbol{x}_f$ [17].

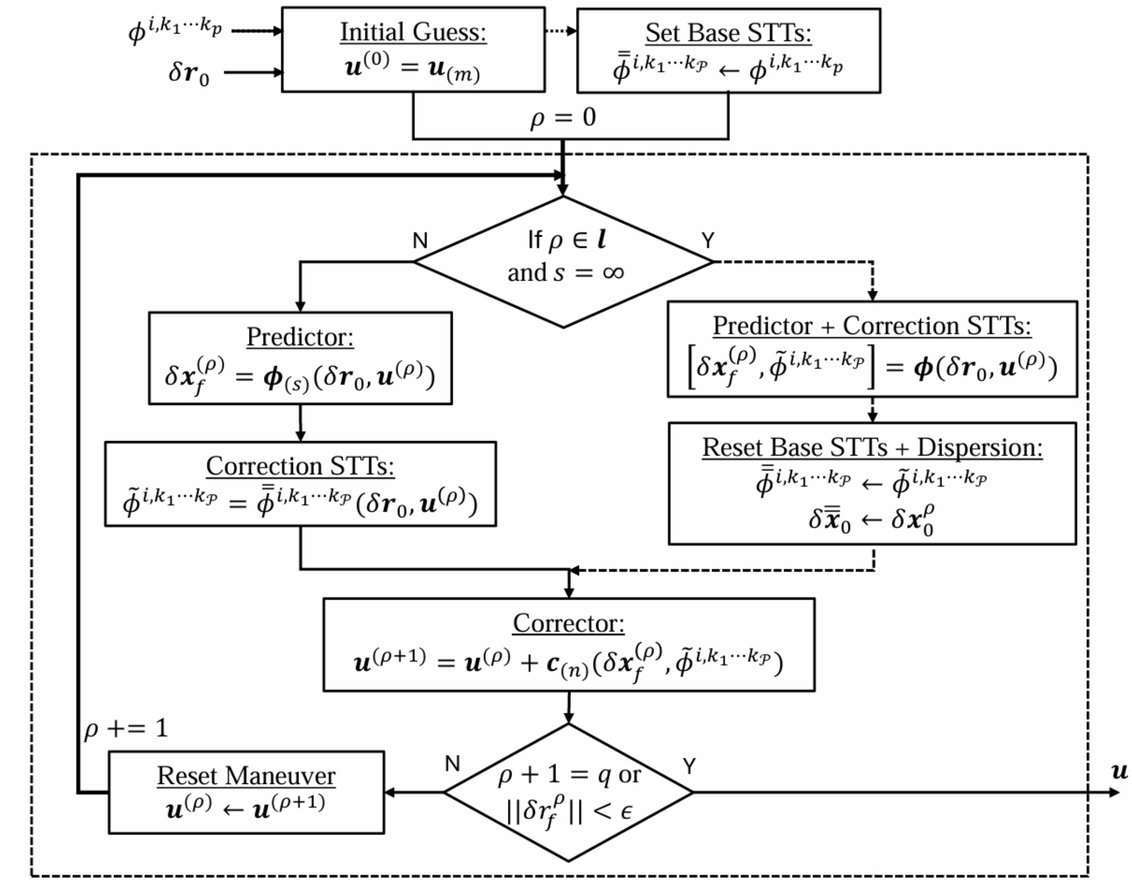

Figure 2: Generalized predictor-corrector defined by $\boldsymbol{\xi} = [\boldsymbol{l}_{(\mathcal{P})}, m, n, q, s]$.

The vector $\boldsymbol{\xi}$ defines the settings of the generalized predictor-corrector, adjusting what the output maneuver $\boldsymbol{u}$ is. The individual settings of $\boldsymbol{\xi}$ are summarized in Table 1 and discussed in greater detail in the current and following sections. For the current work, the order p of the reference STTs $\phi^{i,k_1\cdots k_p}$ is an independent variable that the settings $\boldsymbol{\xi}$ are dependent on. Specific effort is dedicated to introduce novel, analytic approximations for certain configurations $\boldsymbol{\xi}$. Many, if not all, defining settings in $\boldsymbol{\xi}$ are interrelated and are discussed in tandem when appropriate.

RECOMPUTING THE BASE STATE TRANSITION TENSORS

The first setting in the generalized predictor-corrector is the set of iterations $\boldsymbol{l}_{(\mathcal{P})}$ at which the base STTs $\bar{\bar{\phi}}^{i,k_1\cdots k_{\mathcal{P}}}$ are recomputed to the $\mathcal{P}$th-order*. Shooting methods classically recalculate the STM at every iteration for a first-order correction [6]; the equivalent setting for the generalized predictor-corrector sets $\boldsymbol{l}$ to include all iterations ρ with $\mathcal{P} = 1$. Never recomputing the base STTs is equivalent to setting $\boldsymbol{l}_{(\mathcal{P})}$ to an empty set. At iterations where the base STTs are not recomputed, the correction STTs $\tilde{\phi}^{i,k_1\cdots k_{\mathcal{P}}}$ are approximated using the base STTs and the base state dispersion

*Figure 2 indicates that the base STTs are only reset if the full dynamics $\boldsymbol{\phi}$, or $s = \infty$, are used. Otherwise, the truncated dynamics $\boldsymbol{\phi}_{(s)}$ are exact and the base STTs never need to be recomputed.

Table 1: Generalized predictor-corrector setting definitions based on reference STTs p.

Terms	Setting $\boldsymbol{\xi} = [\boldsymbol{l}_{(\mathcal{P})}, m, n, q, s]$	Equations	Contribution
Base STTs and dispersion: $\bar{\bar{\phi}}$, $\delta\bar{\bar{\boldsymbol{x}}}_0$	$[\boldsymbol{l}$, -, -, -, -] $\mathcal{P} \leq p$.	Eq. 4	Current work and [16]
Initial Guess: $\boldsymbol{u}_{(m)}$	[-, m, -, -, -] $m \leq p$	Eqs. 5, 7, 10, 12	Current work and [8, 10]
Correction: $\boldsymbol{c}_{(n)}$	[-, -, n, -, -] $n \leq p$	Eqs. 24- 27 Appendix C	Current work and [9, 14]
Max Iteration: q	[-, -, -, q, -]	Eqs. 13- 15	Current work
Dynamics: $\boldsymbol{\phi}_{(s)}$	[-, -, -, -, s] $s \leq p$	Eqs. 2, 16, 17	Current work and [7, 15]

$\delta\bar{\bar{\boldsymbol{x}}}_0$; Equation 4 shows the approximation of the first-order correction STT $\tilde{\phi}^{i,j}$:

$$\tilde{\phi}^{i,j} = \bar{\bar{\phi}}^{i,j} + \sum_{\mathcal{P}=1}^{p-1} \frac{1}{\mathcal{P}!} \bar{\bar{\phi}}^{i,jk_1\cdots k_{\mathcal{P}}} \left(\delta x_0^{k_1} - \delta\bar{\bar{x}}_0^{k_1}\right) \cdots \left(\delta x_0^{k_{\mathcal{P}}} - \delta\bar{\bar{x}}_0^{k_{\mathcal{P}}}\right). \tag{4}$$

The base STTs $\bar{\bar{\phi}}^{i,k_1\cdots k_{\mathcal{P}}}$ are initialized as the reference STTs, see Fig. 2. The base state dispersion $\delta\bar{\bar{\boldsymbol{x}}}_0$ is initialized as the zero vector. At each iteration in $\boldsymbol{l}$, the base STTs are recomputed along the intermediate trajectory and the base state dispersion $\delta\bar{\bar{\boldsymbol{x}}}_0$ is set to the intermediate state dispersion $\delta\boldsymbol{x}_0^{(\rho)}$. The approximation of the correction STTs in Eq. 4 becomes more accurate as the difference between $\delta\boldsymbol{x}_0$ and $\delta\bar{\bar{\boldsymbol{x}}}_0$ shrinks. It is assumed that the base STTs are never recomputed to an order higher than the original reference STTs, i.e., $\mathcal{P} \leq p$.

Recomputing the base STTs at every iteration is the most accurate, but the most computationally expensive setting; never recomputing the base STTs is computationally cheap, but the least accurate [16]. Within the generalized predictor-corrector, the initial position dispersion $\delta\boldsymbol{r}_0$ is constant across all iterations ρ. Upon the first recomputation in $\boldsymbol{l}$, the position elements of $\delta\boldsymbol{x}_0 - \delta\bar{\bar{\boldsymbol{x}}}_0$ in Eq. 4 become the zero vector. As such, recomputing the base STTs just once on the first iteration is an effective and computationally light setting for $\boldsymbol{l}$.

THE INITIAL GUESS AND THE IMPLICIT VALUE THEOREM

In this section the derivation of higher-order guesses, $\boldsymbol{\xi}$ = [-, m, -, -, -], are introduced to the generalized predictor-corrector based on the multivariate implicit value theorem. Expanding upon related works in the literature [8, 10, 14], higher-order impulsive maneuvers are presented and fed as initial guesses to the generalized predictor-corrector. The resulting higher-order guesses can be utilized as non-iterative targeting maneuvers, and to the authors' knowledge do not exist elsewhere in the literature.

The maneuver $\boldsymbol{u}^*$ driving an initial position dispersion $\delta\boldsymbol{r}_0$ back to the reference (depicted in Fig. 3) is the solution of a root-solved process, and has no analytic solution. However, the solution $\boldsymbol{u}^*$ can be expressed with a Taylor series using the sensitivities from the implicit value theorem, as is similarly done for optimal control formulations [8, 10]. This section utilizes the implicit value theorem to approximate the root-solved solution $\boldsymbol{u}^*$, yielding a higher-order guess to the generalized predictor-corrector.

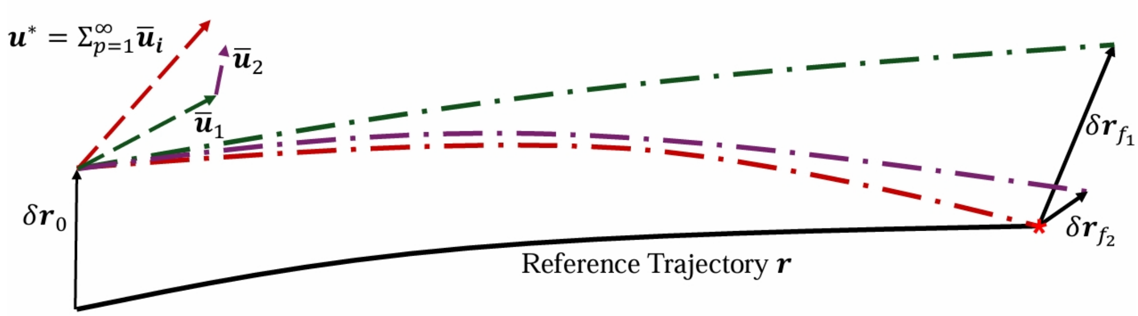

Figure 3: Analytic series approximation of the nonlinear targeting solution $\boldsymbol{u}^*$ with implicit sensitivities.

The root-solved solution $\boldsymbol{u}^*$ is expressed as a Taylor series, where the ith element is expressed as $\bar{\boldsymbol{u}}_i$ [†]:

$$\boldsymbol{u}^*(\delta\boldsymbol{r}_0) = \sum_{i=1}^{\infty} \bar{\boldsymbol{u}}_i(\delta\boldsymbol{r}_0). \tag{5}$$

The first term $\bar{\boldsymbol{u}}_1$ is widely recognized as the solution to the first-order dynamics [1], expressed as a function of the reference STM:

$$\bar{\boldsymbol{u}}_1 = -\boldsymbol{\Phi}_{\boldsymbol{rv}}^{-1}\boldsymbol{\Phi}_{\boldsymbol{rr}}\delta\boldsymbol{r}_0. \tag{6}$$

The higher-order terms $\bar{\boldsymbol{u}}_i$ improve the approximation of the root-solved solution $\boldsymbol{u}^*$ via the higher-order implicit sensitivities [8], derived in the next section for the impulsive nonlinear targeting problem. Just as the first-order maneuver in Eq. 6 is commonly implemented as an initial guess to shooting methods [15], Eq. 5 can be truncated to the mth order, defining a *higher-order guess* for the generalized predictor-corrector:

$$\boldsymbol{u}_{(m)}(\delta\boldsymbol{r}_0) := \sum_{i=1}^{m} \bar{\boldsymbol{u}}_i(\delta\boldsymbol{r}_0). \tag{7}$$

A higher-order guess $\boldsymbol{u}_{(m)}$ decreases the final position dispersion $\delta\boldsymbol{r}_f$, illustrated in Fig. 3. Within the context of the generalized predictor-corrector, setting the higher-order guess to m and performing no iterations ($q = 0$) is usually the cheapest computationally. Just as first-order targeting methods are frequently implemented for autonomous implementation [1, 2], a higher-order guess $m > 1$ outperforms first-order targeting maneuvers.

In summary, setting the generalized predictor-corrector $\boldsymbol{\xi} = [\boldsymbol{l}_{(\mathcal{P})}, m, n, q, s]$ to [-, m, -, 0, -] introduces a targeting method dubbed *higher-order implicit targeting*. The existence of the higher-order implicit targeting strategy in Eq. 7 elsewhere is unknown to the authors; other forms of analytic higher-order guidance methods in the literature attempt to deviate from the reference, reaching a new final target state [14, 18]. Provided the reference STTs are available up to order p, the computational cost of computing $\boldsymbol{u}_{(m)}$ up to $m = p$ is negligible.

[†]The root-solved solution $\boldsymbol{u}^*$ can be directly found via Eq. 5, but requires the reference STTs up to an intractable order; it is more practical to use shooting methods.

Implicit Sensitivities of Root-Solved Processes

Here, the derivation of the implicit sensitivities of the root-solved solution $\boldsymbol{u}^*$ is presented in the context of the BVP solved with an impulsive maneuver; for further reading on the implicit value theorem see [8, 10, 14]. Consider the final state dispersion $\delta\boldsymbol{r}_f$ based on the nonlinear position dynamics $\boldsymbol{\phi}_{\boldsymbol{r}}$ (found by numerically integrating the full state ODEs and extracting the final position components), an initial dispersion $\delta\boldsymbol{r}_0$, and the nonlinear targeting solution $\boldsymbol{u}^*$ defined as a function implicit on $\delta\boldsymbol{r}_0$:

$$\delta\boldsymbol{r}_f = \boldsymbol{\phi}_{\boldsymbol{r}}\left(\delta\boldsymbol{r}_0, \boldsymbol{u}^*(\delta\boldsymbol{r}_0)\right). \tag{8}$$

To compute the sensitivities of $\boldsymbol{u}^*$ with respect to $\delta\boldsymbol{r}_0$, the partials of the final position $\delta\boldsymbol{r}_f$ are taken with respect to the initial position $\delta\boldsymbol{r}_0$, isolating the targeting sensitivities.

The first-order targeting sensitivity matrix $u_r^{*i,j}$ is found by taking the partial of Eq. 8 with respect to the position, yielding

$$\frac{\partial \delta r_f^i}{\partial \delta r_0^j} = \phi_{r,r}^{i,j} + \phi_{r,v}^{i,\alpha} u_r^{*\alpha,j}. \tag{9}$$

The solution $\boldsymbol{u}^*$ reaches the final target by definition, such that $\delta\boldsymbol{r}_f$ is always zero. The derivative of zero is also zero. Therefore, Eq. 9 is set to zero to isolate the first-order targeting sensitivity:

$$u_r^{*i,j} = -\left[\phi_{r,v}^{-1}\right]^{i,\alpha} \phi_{r,r}^{\alpha,j}. \tag{10}$$

Note that Eq. 10 matches the first-order partial of the first-order targeting method in Eq. 6. Just as Eq. 9 is equal to zero, all higher-order sensitivities of $\delta\boldsymbol{r}_f$ to $\delta\boldsymbol{r}_0$ are equal to zero, and the higher-order targeting sensitivities can be isolated. The second-order targeting sensitivity $u_{rr}^{*i,jk}$ is found by differentiating Eq. 9 again

$$\frac{\partial^2 \delta r_f^i}{\partial \delta r_0^j \partial \delta r_0^k} = \phi_{r,rr}^{i,jk} + \phi_{r,rv}^{i,j\alpha} u_r^{*\alpha,k} + \phi_{r,vr}^{i,\alpha k} u_r^{*\alpha,j} + \phi_{r,vv}^{i,\alpha\beta} u_r^{*\alpha,j} u_r^{*\beta,k} + \phi_{r,v}^{i,\alpha} u_{rr}^{*\alpha,jk}, \tag{11}$$

leading to the second-order targeting tensor

$$u_{rr}^{*i,jk} = -\left[\phi_{r,v}^{-1}\right]^{i,\alpha} \left(\phi_{r,rr}^{\alpha,jk} + \phi_{r,rv}^{\alpha,j\beta} u_r^{*\beta,k} + \phi_{r,vr}^{\alpha,\beta k} u_r^{*\beta,j} + \phi_{r,vv}^{\alpha,\beta\gamma} u_r^{*\beta,j} u_r^{*\gamma,k}\right). \tag{12}$$

Note that the second-order targeting sensitivity $u_{rr}^{*i,jk}$ has several first-order sensitivities embedded. The second-order targeting sensitivity yields $\bar{\boldsymbol{u}}_2$ in the Taylor series expansion of $\boldsymbol{u}^*$ in Eq. 5. The higher-order targeting sensitivities are found by repeating the process presented in Eqs. 9-12; the third- and fourth-order targeting sensitivities are presented in Appendix B as Eqs. 22-23. The higher-order targeting sensitivities presented in Eqs. 10, 12, 22, and 23 are new contributions for the impulsive BVP formulation. Again, provided the reference STTs are available, the computational cost of $\boldsymbol{u}_{(m)}$ is negligible.

For the generalized predictor-corrector, feeding a higher-order implicit guess $\boldsymbol{u}_{(m)}$ reduces the number of necessary iterations ρ and expands the region of convergence as a function of $\delta\boldsymbol{r}_0$ [8, 10]. Specifically, implementing a higher-order guess m reduces the number of necessary iterations by approximately m: this relation is introduced more thoroughly in a later section. In instances where $\delta\boldsymbol{r}_0$ is very large, a higher-order guess $\boldsymbol{u}_{(m)}$ may be necessary to ensure the predicted final dispersion $\delta\boldsymbol{r}_f$ reduces to levels appropriately captured by the correction step $\boldsymbol{c}_{(n)}$.

CORRECTION ORDER

In this section, the higher-order correction $\boldsymbol{c}_{(n)}$ is discussed for the generalized predictor-corrector, or $\boldsymbol{\xi} = [\text{-}, \text{-}, n, \text{-}, \text{-}]$. Higher-order corrections are presented in existing literature using a series reversion [9, 14]. The primary contribution in the current work with respect to the correction order is an alternative derivation based on the implicit value theorem and the inverse properties of the STTs [17], presented in Appendix C. Additional contributions from the current work include the incorporation of the correction order in the generalized predictor-corrector and a discussion of its relationship to the other settings in $\boldsymbol{\xi}$.

The higher-order correction $\boldsymbol{c}_{(n)}$ requires the STTs up to order n; thus, the generalized predictor-corrector is restricted by the $\mathcal{P}$th-order base STTs according to $n \leq \mathcal{P}$. At iterations where the correction STTs are approximated using Eq. 4, higher-order corrections must be implemented cautiously; the approximation errors of the correction STTs $\tilde{\phi}^{i,k_1\cdots k_{\mathcal{P}}}$ from Eq. 4 are compounded within the correction $\boldsymbol{c}_{(n)}$ as n increases. If the generalized predictor-corrector is set to have truncated dynamics $\boldsymbol{\phi}_{(s)}$, where s is set to p based on the provided reference STTs, the correction step $\boldsymbol{c}_{(n)}$ can be utilized fully to $n = s = p$.

MAX ITERATION

The impact of the maximum number of iterations q, or $\boldsymbol{\xi} = [\text{-}, \text{-}, \text{-}, q, \text{-}]$, is discussed in the current section. Imposing a maximum number of iterations in shooting methods and root-solvers is ubiquitous. Contributions from the current work are dedicated to studying the relationship between the number of iterations and the implicit sensitivities, specifically with respect to the first iteration and initial guess.

Generally, setting the maximum number of iterations q to a large number, or infinity, will drive the final position error $\delta\boldsymbol{r}_f$ to zero. As discussed previously, setting $q = 0$ utilizes the initial guess as the targeting solution. Setting $q = 1$ performs a single iteration, improving the initial guess based on the final dispersion $\delta\boldsymbol{r}_f$. The intermediate solution after the first iteration is denoted as $\boldsymbol{u}^{(1)}$. An analytic approximation of $\boldsymbol{u}^{(1)}$ is found utilizing the implicit sensitivities derived previously.

The maneuver corrected after one iteration $\boldsymbol{u}^{(1)}$ is expressed as a function of the initial guess $\boldsymbol{u}_{(m)}$ and the correction $\boldsymbol{c}_{(n)}$ according to

$$\boldsymbol{u}^{(1)} = \boldsymbol{u}_{(m)}(\delta\boldsymbol{r}_0) + \boldsymbol{c}_{(n)}(\delta\boldsymbol{r}_f, \tilde{\phi}^{i,k_1\cdots k_{\mathcal{P}}}), \tag{13}$$

where the correction step is a function of the final state dispersion $\delta\boldsymbol{r}_f$ and the correction STT $\tilde{\phi}^{i,k_1\cdots k_{\mathcal{P}}}$, both of which are implicitly defined as a function of the initial state dispersion and initial guess. Expanding Eq. 13 with a Taylor series using coefficients $\bar{\boldsymbol{u}}_i$ for the initial guess and $\bar{\boldsymbol{c}}_{(n)_i}$ for the correction function, expressing both as functions of the initial dispersion $\delta\boldsymbol{r}_0$, yields

$$\boldsymbol{u}^{(1)}(\delta\boldsymbol{r}_0) = \sum_{i=1}^{m} \bar{\boldsymbol{u}}_i(\delta\boldsymbol{r}_0) + \sum_{i=1}^{\infty} \bar{\boldsymbol{c}}_{(n)_i}(\delta\boldsymbol{r}_0). \tag{14}$$

Taking the partial of $\boldsymbol{c}_{(n)}$ and analyzing at the reference trajectory indicates that all coefficients $\bar{\boldsymbol{c}}_{(n)_i}$ up to $i = m$ are equal to zero, i.e., the initial guess $\boldsymbol{u}_{(m)}$ negates the sensitivities of $\boldsymbol{c}_{(n)}$ up to the mth-order. Furthermore, the $(m+1)$th sensitivity of $\boldsymbol{c}_{(n)}$ is equivalent to $\bar{\boldsymbol{u}}_{m+1}$. Therefore, the expansion in Eq. 14 is re-expressed as

$$\boldsymbol{u}^{(1)}(\delta\boldsymbol{r}_0) = \sum_{i=1}^{m+1} \bar{\boldsymbol{u}}_i(\delta\boldsymbol{r}_0) + \sum_{i=m+2}^{\infty} \bar{\boldsymbol{c}}_{(n)_i}(\delta\boldsymbol{r}_0). \tag{15}$$

Equation 15 applies to all correction orders n and both methods of computing the correction STTs. The generalized predictor-corrector $\boldsymbol{\xi} = [\boldsymbol{l}_{(\mathcal{P})}, m, n, q, s]$ with an initial guess $\boldsymbol{u}_{(m)}$ corrected with a single iteration $\boldsymbol{\xi} = [\text{-}, m, \text{-}, 1, \text{-}]$ has the same analytic expression up to order $m+1$ as $\boldsymbol{\xi} = [\text{-}, m+1, \text{-}, 0, \text{-}]$. Equation 15 indicates that an mth-ordered initial guess essentially reduces the necessary number of iterations ρ in the predictor-corrector by m.

ORDER OF DYNAMICS

Replacing the exact, numerically integrated nonlinear dynamics $\boldsymbol{\phi}$ (alternatively denoted as $s = \infty$) with the Taylor series $\boldsymbol{\phi}_{(s)}$ is originally introduced by Park and Scheeres [7] and expanded by Boone and McMahon [15]. The current work incorporates the truncated dynamics into the generalized predictor-corrector, or $\boldsymbol{\xi} = [\text{-}, \text{-}, \text{-}, \text{-}, s]$. Furthermore, analytic approximations to the root-solved solution $\boldsymbol{\sigma}^*_{(s)}$ satisfying the truncated dynamics $\boldsymbol{\phi}_{(s)}$ are introduced using the implicit sensitivities.

As $\boldsymbol{\sigma}^*_{(s)}$ is the solution of a root-solved process, the implicit sensitivities are implemented in similar fashion to the full nonlinear targeting solution $\boldsymbol{u}^*$. The series expansion of $\boldsymbol{\sigma}^*_{(s)}$ is expressed with individual terms $\bar{\boldsymbol{\sigma}}_{(s)_i}$ as[‡]

$$\boldsymbol{\sigma}^*_{(s)}(\delta \boldsymbol{r}_0) = \sum_{i=1}^{\infty} \bar{\boldsymbol{\sigma}}_{(s)_i}(\delta \boldsymbol{r}_0). \tag{16}$$

The implicit sensitivities for $\boldsymbol{\sigma}^*_{(s)_i}$ are found via Eqs. 9-12, including STTs up to the sth order. The coefficients $\bar{\boldsymbol{u}}_i$ in Eq. 5 are equivalent to $\bar{\boldsymbol{\sigma}}_{(s)_i}$ for $i \leq s$, meaning Eq. 16 can be alternatively expressed as

$$\boldsymbol{\sigma}^*_{(s)}(\delta \boldsymbol{r}_0) = \sum_{i=1}^{s} \bar{\boldsymbol{u}}_i(\delta \boldsymbol{r}_0) + \sum_{i=s+1}^{\infty} \bar{\boldsymbol{\sigma}}_{(s)_i}(\delta \boldsymbol{r}_0). \tag{17}$$

Therefore, the approximation of $\boldsymbol{u}^*$ is equivalent to the approximation of $\boldsymbol{\sigma}^*$ up to the sth-order. The solution $\boldsymbol{\sigma}^*_{(s)}$ is an *exact* solution to the *approximate* dynamics $\boldsymbol{\phi}_{(s)}$, whereas the initial guess $\boldsymbol{u}_{(m)}$ is an *approximation* of the *exact* solution $\boldsymbol{u}^*$.

As solving the sth-order dynamics assumes the reference STTs up to order s are provided, there is no computational burden to compute an initial guess of $\boldsymbol{u}_{(m)}$ for $m = s$. Furthermore, as the dynamics $\boldsymbol{\phi}_{(s)}$ are an analytic expression of the STTs, there is no computational burden nor loss in accuracy by implementing a higher-order correction $\boldsymbol{c}_{(n)}$ up to $n = s$. In other words, the general predictor-corrector setting $\boldsymbol{\xi}$ should always be set such that $m = n = s$ (for s not equal to infinity).

NONLINEAR TARGETING ANALYSIS EXAMPLE

The generalized predictor-corrector and its settings $\boldsymbol{\xi}$ are demonstrated for a targeting problem in a circular, polar orbit about Psyche, see Fig. 4. The orbit has an initial semi-major axis of $a_0 = 400$ km. The nominal orbit is modeled with a 3×3 gravity field. The gravity field of Psyche is currently unknown, but the J_2 and C_{22} coefficients are readily produced from the current shape model provided by Shepard [19, 20]. For simplicity, the third-order cosine coefficients from Vesta are implemented; Vesta's gravity field is well modeled [21] and hypothesized to be similar to

[‡]Like $\boldsymbol{u}^*$ in Eq. 5, the root-solved solution $\boldsymbol{\sigma}^*_{(s)}$ can be directly found via Eq. 16, but unlike $\boldsymbol{u}^*$ only requires the reference STTs up to s.

Psyche [22]. The physical constants used in the current work are reported in Table 2. The nominal model assumes Psyche is a principal axis spinner, with a right-ascension of $\alpha = 34°$, declination $\delta = -7°$, and spin rate $\dot{\theta} = 85.8°$ / hr [19]. The targeting scenarios seek to return to the final position after a 24 hour window, or approximately two revolutions.

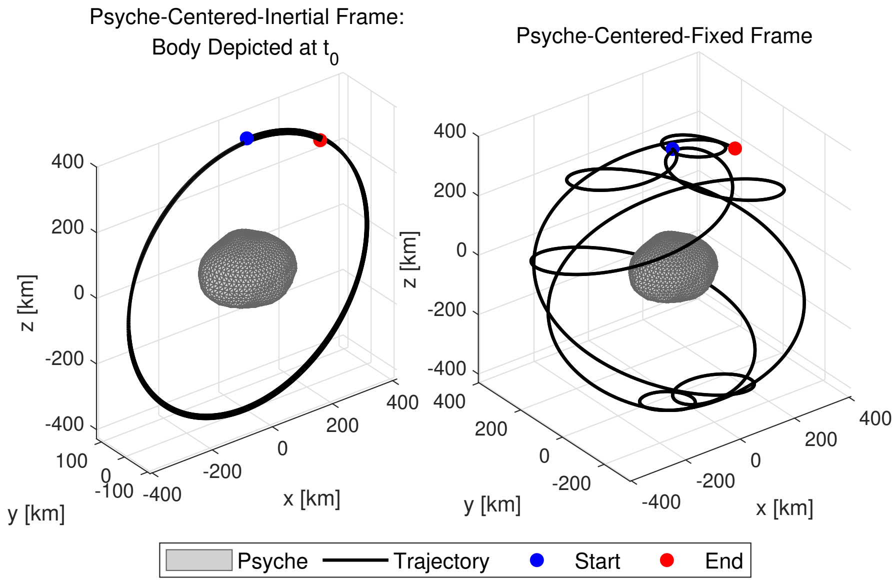

Figure 4: Nominal Psyche orbit over 24 hours.

Table 2: Physical constants used for Psyche simulation.

Parameter	μ [km^3/s^2]	J_2 [-]	C_{22} [-]	J_3 [-]	C_{31} [-]	C_{32} [-]	C_{33} [-]
	1.601	1.03×10^{-1}	1.91×10^{-2}	-8.75×10^{-3}	2.38×10^{-2}	7.60×10^{-5}	4.63×10^{-5}

Higher-Order Initial Guesses

In the first example, the initial guess of the generalized predictor-corrector with no iterations, or $\boldsymbol{\xi} = [\boldsymbol{l}_{(\mathcal{P})}, m, n, q, s] = [\text{-}, m, \text{-}, 0, \text{-}]$ is studied. Ten thousand position dispersions $\delta \boldsymbol{r}_0$ are generated from an initial covariance for a Monte Carlo study. Within the Radial, In-Track, Cross-Track (RIC) frame, the initial dispersion covariance is diagonal with standard deviations of $\{5, 10, 5\}$ km, with a zero-mean initial dispersion. Using the implicit sensitivities, the higher-order guesses $\boldsymbol{u}_{(m)}$ are calculated up to $m = 4$; the initial state dispersion and targeting solution are then propagated forward to the final time.

The final position dispersions are depicted in Fig. 5 for each Monte Carlo sample. The final position dispersions decrease as the order of the initial guess m increases. Furthermore, the average error between the initial guess $\boldsymbol{u}_{(m)}$ and the root-solved solution $\boldsymbol{u}^*$ decreases as m increases. The most significant improvement is seen between $m = 1$ and $m = 2$. The computation time of the generalized predictor-correction increases as the order m increases, but up to fourth-order is less than 5 ms on average[§].

[§]All code presented in the current work is run with MATLAB, on a laptop with 1 CPU with a 1.4 GHz processor.

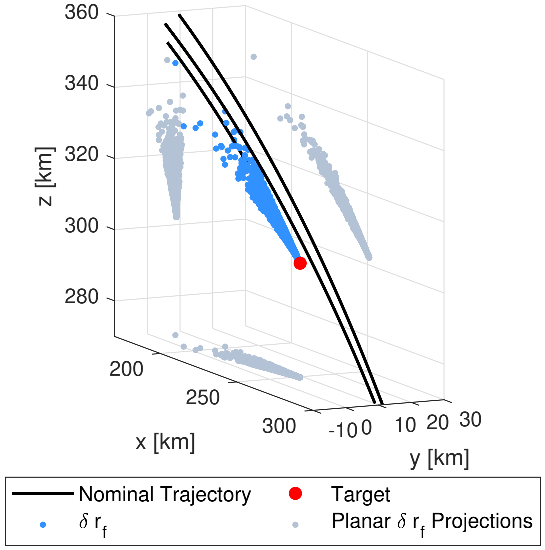

(a) Implicit targeting $\boldsymbol{u}_{(1)}$ performance:
$\boldsymbol{\xi} = [\boldsymbol{l}_{(\mathcal{P})}, m, n, q, s] = [\text{-}, 1, \text{-}, 0, \text{-}]$,
mean miss $||\delta \boldsymbol{r}_f|| = 8.77$ km,
relative $\boldsymbol{u}^*$ error $= 3.12\%$,
average targeting runtime $= 0.25$ ms.

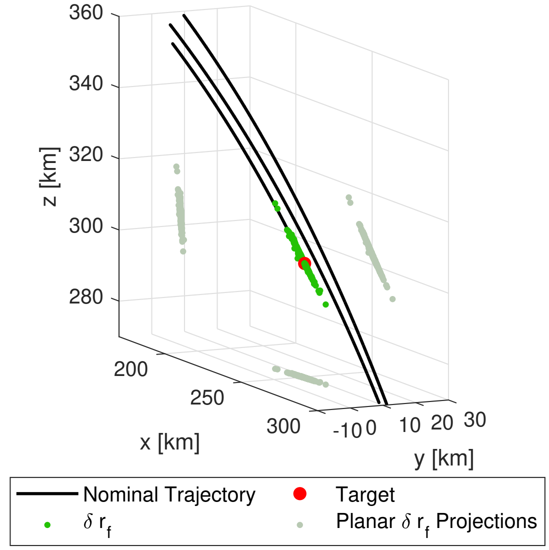

(b) Implicit targeting $\boldsymbol{u}_{(2)}$ performance:
$\boldsymbol{\xi} = [\boldsymbol{l}_{(\mathcal{P})}, m, n, q, s] = [\text{-}, 2, \text{-}, 0, \text{-}]$,
mean miss $||\delta \boldsymbol{r}_f|| = 0.60$ km,
relative $\boldsymbol{u}^*$ error $= 0.32\%$,
average targeting runtime $= 0.98$ ms.

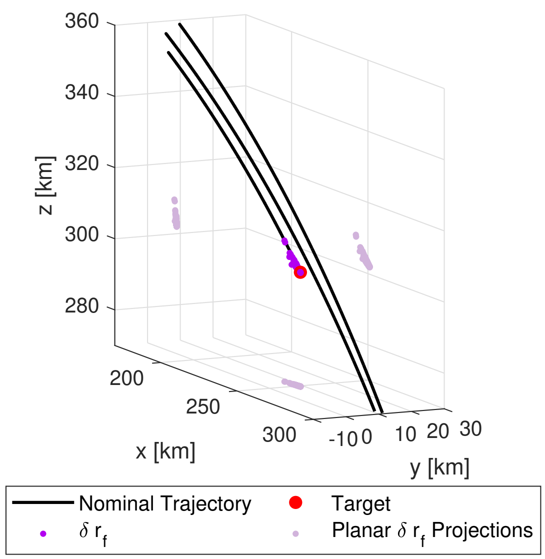

(c) Implicit targeting $\boldsymbol{u}_{(3)}$ performance:
$\boldsymbol{\xi} = [\boldsymbol{l}_{(\mathcal{P})}, m, n, q, s] = [\text{-}, 3, \text{-}, 0, \text{-}]$,
mean miss $||\delta \boldsymbol{r}_f|| = 0.18$ km,
relative $\boldsymbol{u}^*$ error $= 0.16\%$,
average targeting runtime $= 1.28$ ms.

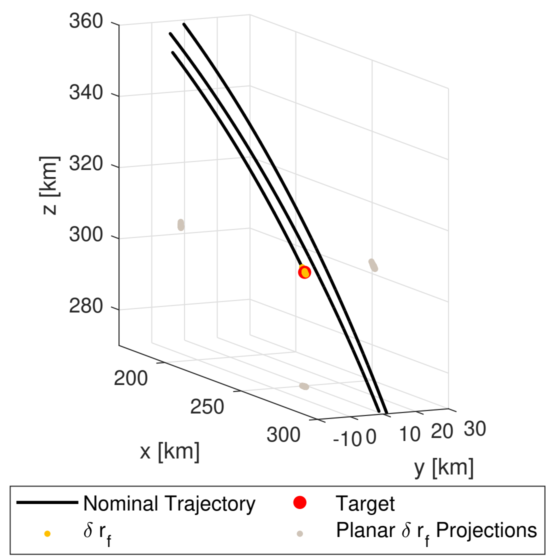

(d) Implicit targeting $\boldsymbol{u}_{(4)}$ performance:
$\boldsymbol{\xi} = [\boldsymbol{l}_{(\mathcal{P})}, m, n, q, s] = [\text{-}, 4, \text{-}, 0, \text{-}]$,
mean miss $||\delta \boldsymbol{r}_f|| = 0.02$ km,
relative $\boldsymbol{u}^*$ error $= 0.05\%$,
average targeting runtime $= 4.18$ ms.

Figure 5: Generalized predictor-corrector $\boldsymbol{\xi} = [\boldsymbol{l}_{(\mathcal{P})}, m, n, q, s] = [\text{-}, m, \text{-}, 0, \text{-}]$; impact of initial guess $\boldsymbol{u}_{(m)}$ on final state dispersions $\delta \boldsymbol{r}_f$.

The mean of $\boldsymbol{u}^*$ is computed empirically from the Monte Carlo samples. An analytic approximation of the empirical mean is computed using the higher-order implicit partials and Gaussian statistics. The predicted means from a second- and fourth-order mapping are compared to the empirical mean, recorded in the RIC frame in Table 3. The first- and third-order means are omitted in Table 3 as the initial state distribution is zero-mean; see the nonlinear mapping of Gaussian variables [7].

Table 3: Analytic and empirical mean of $\boldsymbol{u}^*$.

	Second-order mean	Fourth-order mean	Empirical mean
Radial [mm/s]	-36.94	-34.24	-34.15
In-Track [mm/s]	-14.11	-17.42	-17.21
Cross-Track [mm/s]	6.85	7.48	7.46

Next, the impact of the higher-order guess $\boldsymbol{u}_{(m)}$ is compared against the higher-order correction $\boldsymbol{c}_{(n)}$ on subsequent iterations of the generalized predictor-corrector. The average miss distance $||\delta \boldsymbol{r}_f||$ over iterations ρ up to $q = 5$ is depicted in Fig. 6. For the first case, depicted in Fig. 6a, the correction step is fixed to $n = 1$ and the initial guess m is modified; the correction STTs $\tilde{\phi}^{i,k_1\cdots k_{\mathcal{P}}}$ are recomputed at every iteration to first-order $\boldsymbol{l}_{(\mathcal{P})} = \{0:1:q\}_{(1)}$. In the second case, depicted in Fig. 6b, the correction step n is modified and the initial guess fixed to $m = 1$; the correction STTs are recomputed at each iteration up to order $\mathcal{P} = n$.

From the results in Fig. 6, the higher-order guess is demonstrated to have a greater impact on reducing the final position dispersion than the higher-order correction. Comparing the cases where $m = n$, each iteration's final position error is smaller in Fig. 6a than in Fig. 6b—except for $m = n = 1$, where the generalized predictor-corrector settings are identical. The benefit of the higher-order correction decreases past the first iteration as $\delta \boldsymbol{r}_f$ decreases.

Recomputing the Correction STTs

Consider again the initial state dispersion defined by $\{5, 10, 5\}$ km in the RIC frame. The first scenario assumes that only the first-order reference STTs are available, $p = 1$, and subsequently computes the first-order guess $\boldsymbol{u}_{(1)}$. One setting never recomputes the base STTs, leading to $\boldsymbol{\xi} = [\boldsymbol{l}_{(\mathcal{P})}, m, n, q, s] = [\{\text{-}\}_{(1)}, 1, 1, 5, \infty]$; the second setting recomputes the base STTs immediately at $\rho = 0$, or $\boldsymbol{\xi} = [\boldsymbol{l}_{(\mathcal{P})}, m, n, q, s] = [\{0\}_{(1)}, 1, 1, 5, \infty]$. The average final position error across iterations ρ is depicted in Fig. 7a. By recomputing the base STTs just once, the final position errors decrease by two orders of magnitude. The same study is expanded to second-order, computing the second-order initial guess $\boldsymbol{u}_{(2)}$ and recomputing the base STTs up to order $\mathcal{P} = 2$. As seen in Fig. 7b, recomputing the base STTs immediately to second-order decreases the final state errors by almost five orders of magnitude.

Truncated Dynamics and Single-Iteration Targeting

Now consider a smaller initial state dispersion defined by the initial standard deviations $\{1, 2, 1\}$ km in the RIC frame. First, the initial guess targeting strategy, up to second-order, is performed; $\boldsymbol{\xi} = [\boldsymbol{l}_{(\mathcal{P})}, m, n, q, s] = [\text{-}, 1, \text{-}, 0, \text{-}]$ for first-order $\boldsymbol{u}_{(1)}$ and $\boldsymbol{\xi} = [\boldsymbol{l}_{(\mathcal{P})}, m, n, q, s] = [\text{-}, 2, \text{-}, 0, \text{-}]$ for second-order $\boldsymbol{u}_{(2)}$. The final state dispersions and targeting information are shown in Figs. 8a and 8b.

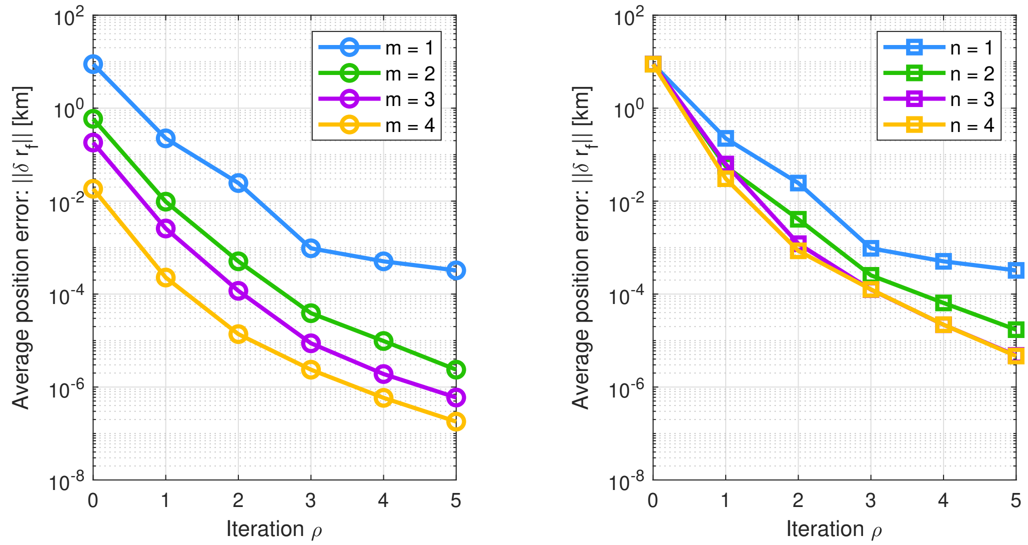

(a) Modifying the initial guess $\boldsymbol{u}_{(m)}$:
$\boldsymbol{\xi} = [\boldsymbol{l}_{(\mathcal{P})}, m, n, q, s] = [\{0\!:\!1\!:\!q\}_{(1)}, m, 1, 5, \infty]$.

(b) Modifying the correction step $\boldsymbol{c}_{(n)}$:
$\boldsymbol{\xi} = [\boldsymbol{l}_{(\mathcal{P})}, m, n, q, s] = [\{0\!:\!1\!:\!q\}_{(n)}, 1, n, 5, \infty]$.

Figure 6: Impact of initial guess vs. correction step.

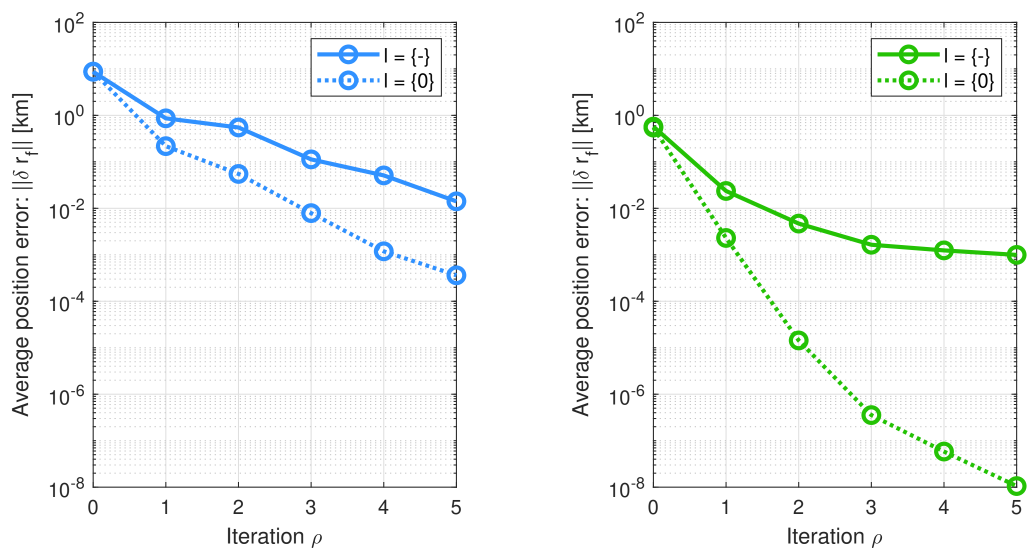

(a) Recomputing the base STTs given ($p = 1$):
$\boldsymbol{\xi} = [\boldsymbol{l}_{(\mathcal{P})}, m, n, q, s] = [\boldsymbol{l}_{(1)}, 1, 1, 5, \infty]$.

(b) Recomputing the base STTs given ($p = 2$):
$\boldsymbol{\xi} = [\boldsymbol{l}_{(\mathcal{P})}, m, n, q, s] = [\boldsymbol{l}_{(2)}, 2, 1, 5, \infty]$.

Figure 7: Recomputing the base STTs once at $\rho = 0$ improves targeting performance.

Next, the generalized predictor-corrector is set to perform a single iteration based on a first-order initial guess using a recomputed STM, or $\boldsymbol{\xi} = [\boldsymbol{l}_{(\mathcal{P})}, m, n, q, s] = [\{0\}_{(1)}, 1, 1, 1, \infty]$. The final state dispersions and targeting information are shown in Fig. 8c. Lastly, the generalized predictor-corrector is set to find the root-solved solution to the second-order dynamics $\boldsymbol{\phi}_{(2)}$, yielding $\boldsymbol{\sigma}^*_{(2)}$, or $\boldsymbol{\xi} = [\boldsymbol{l}_{(\mathcal{P})}, m, n, q, s] = [\text{-}, 2, 1, 5, 2]$. Note that the recomputation setting $\boldsymbol{l}_{(\mathcal{P})}$ is irrelevant for truncated dynamics, see Fig. 2. The final position dispersions arising from $\boldsymbol{\sigma}^*_{(2)}$ are shown in Fig. 8d.

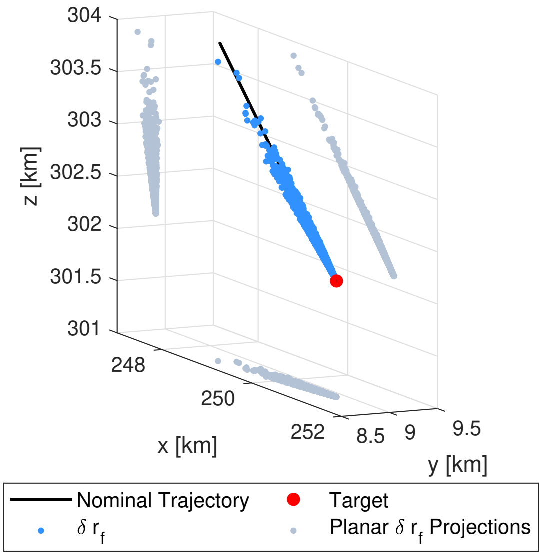

(a) Implicit targeting $\boldsymbol{u}_{(1)}$ performance:
$\boldsymbol{\xi} = [\boldsymbol{l}_{(\mathcal{P})}, m, n, q, s] = [\text{-}, 1, \text{-}, 0, \text{-}]$,
mean miss $||\delta \boldsymbol{r}_f|| = 350.5$ m,
relative $\boldsymbol{u}^*$ error $= 0.64\%$,
average targeting runtime $= 0.25$ ms.

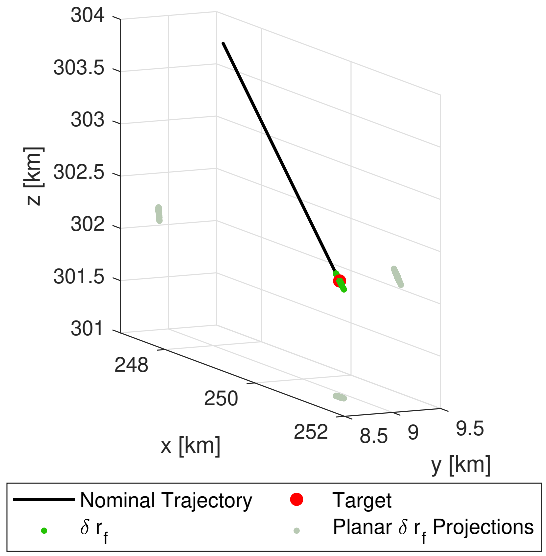

(b) Implicit targeting $\boldsymbol{u}_{(2)}$ performance:
$\boldsymbol{\xi} = [\boldsymbol{l}_{(\mathcal{P})}, m, n, q, s] = [\text{-}, 2, \text{-}, 0, \text{-}]$,
mean miss $||\delta \boldsymbol{r}_f|| = 4.6$ m,
relative $\boldsymbol{u}^*$ error $= 0.01\%$,
average targeting runtime $= 0.98$ ms.

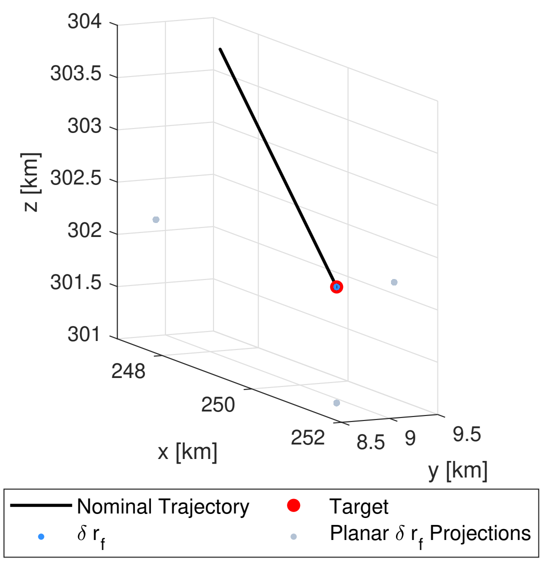

(c) Single-iteration $\boldsymbol{u}^{(1)}$ performance:
$\boldsymbol{\xi} = [\boldsymbol{l}_{(\mathcal{P})}, m, n, q, s] = [\{0\}_{(1)}, 1, 1, 1, \infty]$,
mean miss $||\delta \boldsymbol{r}_f|| = 0.3$ m,
relative $\boldsymbol{u}^*$ error $= 0.14\%$,
average targeting runtime $= 58.09$ ms.

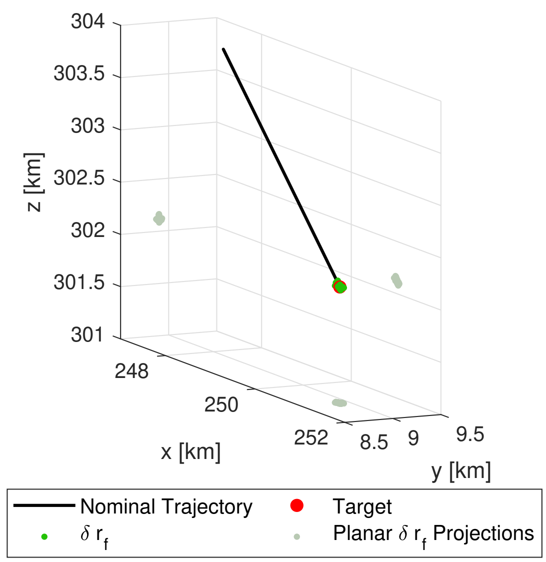

(d) Truncated dynamics $\boldsymbol{\sigma}^*_{(2)}$ performance:
$\boldsymbol{\xi} = [\boldsymbol{l}_{(\mathcal{P})}, m, n, q, s] = [\text{-}, 2, 1, 5, 2]$,
mean miss $||\delta \boldsymbol{r}_f|| = 4.1$ m,
relative $\boldsymbol{u}^*$ error $= 0.12\%$,
average targeting runtime $= 1.07$ ms.

Figure 8: Comparing similar targeting strategies based on the second-order implicit sensitivities.

According to Eq. 15 and Eq. 17, both the first iteration solution $\boldsymbol{u}^{(1)}$ based on a first-order initial guess and the root-solved solution of the second-order dynamics $\boldsymbol{\sigma}^*_{(2)}$ have the same second-order approximation as $\boldsymbol{u}_{(2)}$. As such, the final position dispersions recorded in Figs. 8b, 8c, and 8d are comparable. The mean of the targeting solutions $\boldsymbol{u}^{(1)}$ and $\boldsymbol{\sigma}^*_{(2)}$ can thus be approximated to second-order using the implicit sensitivities, shown in Table 4.

Table 4: Second-order approximation against empirical means of $\boldsymbol{u}^{(1)}$ and $\boldsymbol{\sigma}^*_{(2)}$.

	Second-order mean	Empirical mean of $\boldsymbol{u}^{(1)}$ $\boldsymbol{\xi} = [\{0\}_{(1)}, 1, 1, 1, \infty]$	Empirical mean of $\boldsymbol{\sigma}^*_{(2)}$ $\boldsymbol{\xi} = [\text{-}, 2, 1, 5, 2]$
Radial [mm/s]	-1.48	-1.51	-1.39
In-Track [mm/s]	-0.56	-0.55	-0.61
Cross-Track [mm/s]	0.27	0.30	0.26

CONCLUSION

The generalized predictor-corrector combines existing contributions from the literature with analytic approximations introduced in the current work to produce an adjustable nonlinear targeting algorithm. The higher-order implicit sensitivities from the root-solved procedure yield higher-order guesses, significantly driving down final state dispersions. The sensitivities provide analytic approximations of nonlinear targeting solutions produced by the generalized predictor-corrector in various scenarios, reducing the number of necessary iterations. Against comparable settings of the generalized predictor-corrector, the analytic implicit sensitivities provide similar final state dispersions for a fraction of the computation cost.

ACKNOWLEDGMENTS

The research is funded by Intuitive Machines, 3700 Bay Area Blvd #600, Houston, TX 77058.

APPENDIX A: STT INTEGRATION

The propagation of the STTs up to fourth-order are a function of the STTs $\phi^{i,k_1\cdots k_p}$ and the partials of the differential equations $f^{i,k_1\cdots k_p}$ [7]:

$$\dot{\phi}^{i,a} = f^{i,\alpha}\phi^{\alpha,a} \tag{18}$$

$$\dot{\phi}^{i,ab} = f^{i,\alpha}\phi^{\alpha,ab} + f^{i,\alpha\beta}\phi^{\alpha,a}\phi^{\beta,b} \tag{19}$$

$$\dot{\phi}^{i,abc} = f^{i,\alpha}\phi^{\alpha,abc} + f^{i,\alpha\beta}\left(\phi^{\alpha,a}\phi^{\alpha,bc} + \phi^{\alpha,ab}\phi^{\beta,c} + \phi^{\alpha,ac}\phi^{\beta,b}\right) + f^{i,\alpha\beta\gamma}\phi^{\alpha,a}\phi^{\beta,b}\phi^{\gamma,c} \tag{20}$$

$$\begin{aligned}\dot{\phi}^{i,abcd} &= f^{i,\alpha}\phi^{\alpha,abcd} + f^{i,\alpha\beta}\Big(\phi^{\alpha,abc}\phi^{\beta,d} + \phi^{\alpha,abd}\phi^{\beta,c} + \phi^{\alpha,acd}\phi^{\beta,b} + \phi^{\alpha,ab}\phi^{\beta,cd}\ldots \\ &\quad +\phi^{\alpha,ac}\phi^{\beta,bd} + \phi^{\alpha,ad}\phi^{\beta,bc} + \phi^{\alpha,a}\phi^{\beta,bcd}\Big) + f^{i,\alpha\beta\gamma}\Big(\phi^{\alpha,ab}\phi^{\beta,c}\phi^{\gamma,d} + \phi^{\alpha,ac}\phi^{\beta,b}\phi^{\gamma,d}\ldots \\ &\quad +\phi^{\alpha,ad}\phi^{\beta,b}\phi^{\gamma,c} + \phi^{\alpha,a}\phi^{\beta,bc}\phi^{\gamma,d} + \phi^{\alpha,a}\phi^{\beta,bd}\phi^{\gamma,c} + \phi^{\alpha,a}\phi^{\beta,b}\phi^{\gamma,cd}\Big) \\ &\quad + f^{i,\alpha\beta\gamma\delta}\phi^{\alpha,a}\phi^{\beta,b}\phi^{\gamma,c}\phi^{\delta,d}\end{aligned} \tag{21}$$

APPENDIX B: HIGHER-ORDER IMPLICIT SENSITIVITIES

Following the partials from Eqs. 12, the third-order targeting sensitivity is

$$\begin{aligned} u_{rrr}^{*i,jkl} = - \left[\phi_{r,v}^{-1}\right]^{i,\alpha} \Big(&\phi_{r,rrr}^{\alpha,jkl} + \phi_{r,rrv}^{\alpha,jk\beta} u_r^{*\beta,l} + \phi_{r,rvr}^{\alpha,j\beta l} u_r^{*\beta,k} + \phi_{r,vrr}^{\alpha,\beta kl} u_r^{*\beta,j} + \phi_{r,rvv}^{\alpha,j\beta\gamma} u_r^{*\beta,k} u_r^{*\gamma,l} \\ &+ \phi_{r,vrv}^{\alpha,\beta k\gamma} u_r^{*\beta,j} u_r^{*\gamma,l} + \phi_{r,vvr}^{\alpha,\beta\gamma l} u_r^{*\beta,j} u_r^{*\gamma,k} + \phi_{r,vr}^{\alpha,\beta l} u_{rr}^{*\beta,jk} + \phi_{r,rv}^{\alpha,j\beta} u_{rr}^{*\beta,kl} + \phi_{r,vr}^{\alpha,\beta k} u_{rr}^{*\beta,jl} \\ &+ \phi_{r,vvv}^{\alpha,\beta\gamma\delta} u_r^{*\beta,j} u_r^{*\gamma,k} u_r^{*\delta,l} + \phi_{r,vv}^{\alpha,\beta\gamma} \left[u_{rr}^{*\beta,jl} u_r^{*\gamma,k} + u_r^{*\beta,j} u_{rr}^{*\gamma,kl} + u_{rr}^{*\beta,jk} u_r^{*\gamma,l}\right]\Big). \end{aligned} \tag{22}$$

The fourth-order targeting sensitivity is

$$\begin{aligned} u_{rrrr}^{*i,jkl} = - \left[\phi_{r,v}^{-1}\right]^{i,\alpha} \Big(&\phi_{r,rrrr}^{\alpha,jklm} + \phi_{r,rrrv}^{\alpha,jkl\beta} u_r^{*\beta,m} + \phi_{r,rrvr}^{\alpha,jk\beta m} u_r^{*\beta,l} + \phi_{r,rvrr}^{\alpha,j\beta lm} u_r^{**\beta,k} + \phi_{r,vrrr}^{\alpha,\beta klm} u_r^{*\beta,j} \ldots \\ &+ \phi_{r,rrvv}^{\alpha,jk\beta\gamma} u_r^{*\beta,l} u_r^{*\gamma,m} + \phi_{r,rvrv}^{\alpha,j\beta l\gamma} u_r^{*\beta,k} u_r^{*\gamma,m} + \phi_{r,rvvr}^{\alpha,j\beta\gamma m} u_r^{*\beta,k} u_r^{*\gamma,l} + \phi_{r,vrrv}^{\alpha,\beta kl\gamma} u_r^{*\beta,j} u_r^{*\gamma,m} + \phi_{r,vrvr}^{\alpha,\beta k\gamma m} u_r^{*\beta,j} u_r^{*\gamma,l} \ldots \\ &+ \phi_{r,vvrr}^{\alpha,\beta\gamma lm} u_r^{*\beta,j} u_r^{*\gamma,k} + \phi_{r,rrv}^{\alpha,jk\beta} u_{rr}^{*\beta,lm} + \phi_{r,rvr}^{\alpha,j\beta l} u_{rr}^{*\beta,km} + \phi_{r,rvr}^{\alpha,j\beta m} u_{rr}^{*\beta,kl} + \phi_{r,vrr}^{\alpha,\beta kl} u_{rr}^{*\beta,jm} + \phi_{r,vrr}^{\alpha,\beta km} u_{rr}^{*\beta,jl} \ldots \\ &+ \phi_{r,vrr}^{\alpha,\beta lm} u_{rr}^{*\beta,jk} + \phi_{r,rvvv}^{\alpha,j\beta\gamma\delta} u_r^{*\beta,k} u_r^{*\gamma,l} u_r^{*\delta,m} + \phi_{r,vrvv}^{\alpha,\beta k\gamma\delta} u_r^{*\beta,j} u_r^{*\gamma,l} u_r^{*\delta,m} + \phi_{r,vvrv}^{\alpha,\beta\gamma l\delta} u_r^{*\beta,j} u_r^{*\gamma,k} u_r^{*\delta,m} \ldots \\ &+ \phi_{r,vvvr}^{\alpha,\beta\gamma\delta m} u_r^{*\beta,j} u_r^{*\gamma,k} u_r^{*\delta,l} + \phi_{r,rvv}^{\alpha,j\beta\gamma} \left[u_{rr}^{*\beta,km} u_r^{*\gamma,l} + u_r^{*\beta,k} u_{rr}^{*\gamma,lm} + u_{rr}^{*\beta,kl} u_r^{*\gamma,m}\right] + \phi_{r,vrv}^{\alpha,\beta l\gamma} u_{rr}^{*\beta,jk} u_r^{*\gamma,m} \ldots \\ &+ \phi_{r,vrv}^{\alpha,\beta k\gamma} \left[u_{rr}^{*\beta,jm} u_r^{*\gamma,l} + u_r^{*\beta,j} u_{rr}^{*\gamma,lm} + u_{rr}^{*\beta,jl} u_r^{*\gamma,m}\right] + \phi_{r,vvr}^{\alpha,\beta\gamma l} \left[u_{rr}^{*\beta,jm} u_r^{*\gamma,k} + u_r^{*\beta,j} u_{rr}^{*\gamma,km}\right] \ldots \\ &+ \phi_{r,vvv}^{\alpha,\beta\gamma\delta} \Big[u_{rr}^{*\beta,jm} u_r^{*\gamma,k} u_r^{*\delta,l} + u_r^{*\beta,j} u_{rr}^{*\gamma,km} u_r^{*\delta,l} + u_r^{*\beta,j} u_r^{*\gamma,k} u_{rr}^{*\delta,lm} + u_{rr}^{*\beta,jl} u_r^{*\gamma,k} u_r^{*\delta,m} \ldots \\ &+ u_r^{*\beta,j} u_{rr}^{*\gamma,kl} u_r^{*\delta,m} + u_{rr}^{*\beta,jk} u_r^{*\gamma,l} u_r^{*\delta,m}\Big] + \phi_{r,vvr}^{\alpha,\beta\gamma m} \left[u_{rr}^{*\beta,jl} u_r^{*\gamma,k} + u_r^{*\beta,j} u_{rr}^{*\gamma,kl} + u_{rr}^{*\beta,jk} u_r^{*\gamma,l}\right] \ldots \\ &+ \phi_{r,rv}^{\alpha,j\beta} u_{rrr}^{*\beta,klm} + \phi_{r,vr}^{\alpha,\beta k} u_{rrr}^{*\beta,jlm} + \phi_{r,vr}^{\alpha,\beta l} u_{rrr}^{*\beta,jkm} + \phi_{r,vr}^{\alpha,\beta m} u_{rrr}^{*\beta,jkl} + \phi_{r,vvvv}^{\alpha,\beta\gamma\delta\varepsilon} u_r^{*\beta,j} u_r^{*\gamma,k} u_r^{*\delta,l} u_r^{*\varepsilon,m} \ldots \\ &+ \phi_{r,vv}^{\alpha,\beta\gamma} \Big[u_{rrr}^{*\beta,jlm} u_r^{*\gamma,k} + u_{rr}^{*\beta,jl} u_{rr}^{*\gamma,km} + u_{rr}^{*\beta,jm} u_{rr}^{*\gamma,kl} + u_r^{*\beta,j} u_{rrr}^{*\gamma,klm} + u_{rrr}^{*\beta,jkm} u_r^{*\gamma,l} + u_{rr}^{*\beta,jk} u_{rr}^{*\gamma,lm} \ldots \\ &u_{rrr}^{*\beta,jkl} u_r^{*\gamma,m}\Big]\Big) \end{aligned} \tag{23}$$

APPENDIX C: DERIVATION OF HIGHER-ORDER CORRECTION STEPS

Here, an alternative derivation of the higher-order correction is presented within the framework of the implicit value theorem and the properties of the STTs. The resulting correction step is mathematically equivalent to the literature [9, 14], but is a more intuitive approach within the lens of the multivariate implicit value theorem. Based on the final state dispersion and the inverse dynamics ψ, the implicit value theorem is framed as

$$\delta \boldsymbol{x}_0 = \psi(\delta \boldsymbol{r}_f^*, \delta \boldsymbol{v}_f^*(\delta \boldsymbol{r}_f^*)), \tag{24}$$

where $\delta \boldsymbol{r}_f^* = -\delta \boldsymbol{r}_f$, and $\delta \boldsymbol{v}_f^*$ is the desired final velocity offset implicit on $\delta \boldsymbol{r}_f^*$. Following the derivation of the implicit sensitivities shown previously, the first-order sensitivity of $\delta \boldsymbol{v}_f^*$ with respect to $\delta \boldsymbol{r}_f^*$ is

$$v_{r_f^*}^{*i,j} = - \left[\psi_{r,v}^{-1}\right]^{i,\alpha} \psi_{r,r}^{\alpha,j}. \tag{25}$$

Equation 25 is then mapped backwards to get the sensitivity of $\boldsymbol{u}$ with respect to the final position and apply the correction according to

$$u_{r_f^*}^{i,j} = \psi_{v,r}^{i,j} + \psi_{v,v}^{i,\alpha} v_{r_f^*}^{*\alpha,j}, \tag{26}$$

$$c^i_{(1)}(\delta r^*_f) = u^{i,\alpha}_{r^*_f}\delta \boldsymbol{r}^{*\alpha}_f. \tag{27}$$

Equation 27 is identical to the classic predictor-corrector step [6]. The derivation is then extended to higher-order. For each intermediate step, the STTs are propagated forward and inverted [17]. Next, the higher-order sensitivities of $\delta \boldsymbol{v}^*_f$ with respect to $\delta \boldsymbol{r}^*_f$ are obtained via the implicit value theorem. Lastly, the sensitivities are mapped backwards to obtain the correction sensitivities $u^{i,k_1\cdots k_p}_{r^*_f}$.

REFERENCES

[1] R. H. Battin, *An introduction to the mathematics and methods of astrodynamics*. AIAA, 1999.

[2] D. Geller, D. Woffinden, and C. York, "Generalized Reference Targeting for Spaceflight," *47th Annual American Astronautical Society (AAS) Guidance, Navigation and Control (GN&C) Conference*, No. AAS-25-099, American Astronomical Society, 2025, https://ntrs.nasa.gov/citations/20250000047.

[3] R. P. Russell, "Complete Lambert solver including second-order sensitivities," *Journal of Guidance, Control, and Dynamics*, Vol. 45, No. 2, 2022, pp. 196–212, https://doi.org/10.2514/1.G006089.

[4] J. W. McMahon and D. J. Scheeres, "Linearized Lambert's problem solution," *Journal of Guidance, Control, and Dynamics*, Vol. 39, No. 10, 2016, pp. 2205–2218, https://doi.org/10.2514/1.G000394.

[5] N. Arora, R. P. Russell, N. Strange, and D. Ottesen, "Partial derivatives of the solution to the Lambert boundary value problem," *Journal of Guidance, Control, and Dynamics*, Vol. 38, No. 9, 2015, pp. 1563–1572, https://doi.org/10.2514/1.G001030.

[6] D. C. Chandler and I. E. Smith, "Development of the iterative guidance mode with its application to various vehicles and missions.," *Journal of Spacecraft and Rockets*, Vol. 4, No. 7, 1967, pp. 898–903, https://doi.org/10.2514/3.28985.

[7] R. S. Park and D. J. Scheeres, "Nonlinear mapping of Gaussian statistics: theory and applications to spacecraft trajectory design," *Journal of guidance, Control, and Dynamics*, Vol. 29, No. 6, 2006, pp. 1367–1375, https://doi.org/10.2514/1.20177.

[8] J. L. Junkins, J. D. Turner, and M. Majji, "Generalizations and applications of the lagrange implicit function theorem," *The Journal of the Astronautical Sciences*, Vol. 57, No. 1, 2009, pp. 313–345, https://doi.org/10.1007/BF03321507.

[9] A. B. Younes and J. Turner, "Generalized least squares and Newton's method algorithms for nonlinear root-solving applications," *The Journal of the Astronautical Sciences*, Vol. 60, No. 3, 2013, pp. 517–540, https://doi.org/10.1007/s40295-015-0071-z.

[10] J. Turner, M. Majji, and J. Junkins, "High-order state and parameter transition tensor calculations," *AIAA/AAS Astrodynamics Specialist Conference and Exhibit*, No. AIAA 2008-6453, 2008, https://doi.org/10.2514/6.2008-6453.

[11] A. Evans, R. Armellin, L. Pirovano, and N. Baresi, "High-order guidance for time-optimal low-thrust trajectories with accuracy control," *Journal of Guidance, Control, and Dynamics*, Vol. 47, No. 2, 2024, pp. 279–290, https://doi.org/10.2514/1.G007540,.

[12] P. Di Lizia, R. Armellin, A. Morselli, and F. Bernelli-Zazzera, "High order optimal feedback control of space trajectories with bounded control," *Acta Astronautica*, Vol. 94, No. 1, 2014, pp. 383–394, https://doi.org/10.1016/j.actaastro.2013.02.011.

[13] M. Majji, J. D. Turner, and J. L. Junkins, "Solution of two-point boundary-value problems using Lagrange implicit function theorem," *Journal of guidance, control, and dynamics*, Vol. 32, No. 5, 2009, pp. 1684–1687, https://doi.org/10.2514/1.43024.

[14] D. Griffith, J. Turoner, S. Vadali, and J. Junkins, "Higher order sensitivities for solving nonlinear two-point boundary-value problems," *AIAA/AAS Astrodynamics Specialist Conference and Exhibit*, No. AIAA 5404, 2004, https://doi.org/10.2514/6.2004-5404.

[15] S. Boone and J. McMahon, "Orbital guidance using higher-order state transition tensors," *Journal of Guidance, Control, and Dynamics*, Vol. 44, No. 3, 2021, pp. 493–504, https://doi.org/10.2514/1.G005493.

[16] E. Pellegrini and R. Russell, "Quasi-newton differential dynamic programming for robust low-thrust optimization," *AIAA/AAS Astrodynamics Specialist Conference*, 2012, p. 4425, https://doi.org/10.2514/6.2012-4425.

[17] R. S. Park and D. J. Scheeres, "Nonlinear semi-analytic methods for trajectory estimation," *Journal of guidance, control, and dynamics*, Vol. 30, No. 6, 2007, pp. 1668–1676, https://doi.org/10.2514/1.29106.

[18] J. Kulik, M. Ruth, C. Orton-Urbina, and D. Savransky, "Applications of induced tensor norms to guidance navigation and control," *Journal of Guidance, Control, and Dynamics*, Vol. 48, No. 10, 2025, pp. 2180–2198, https://doi.org/10.2514/1.G009054.

[19] M. K. Shepard, J. Richardson, P. A. Taylor, L. A. Rodriguez-Ford, A. Conrad, I. d. Pater, M. Adamkovics, K. d. Kleer, J. R. Males, K. M. Morzinski, *et al.*, "Radar observations and shape model of asteroid 16 Psyche," *Icarus*, Vol. 281, 2017, pp. 388–403, https://doi.org/10.1016/j.icarus.2016.08.011.

[20] K. Oguri, G. Lantoine, W. Hart, and J. McMahon, "Science orbit design with a quasi-frozen beta angle: effects of body obliquity on J2-perturbed dynamics," *Celestial Mechanics and Dynamical Astronomy*, Vol. 132, No. 10, 2020, p. 48, https://doi.org/10.1007/s10569-020-09987-z.

[21] A. S. Konopliv, S. Asmar, B. Bills, N. Mastrodemos, R. Park, C. Raymond, D. Smith, and M. Zuber, "The Dawn gravity investigation at Vesta and Ceres," *Space Science Reviews*, Vol. 163, No. 1, 2011, pp. 461–486, https://doi.org/10.1007/s11214-011-9794-8.

[22] L. T. Elkins-Tanton, E. Asphaug, J. F. Bell III, C. J. Bierson, B. G. Bills, W. F. Bottke, S. W. Courville, S. D. Dibb, I. Jun, D. J. Lawrence, *et al.*, "Distinguishing the origin of asteroid (16) Psyche," *Space Science Reviews*, Vol. 218, No. 3, 2022, p. 17, https://doi.org/10.1007/s11214-022-00880-9.